Check for updates

{Gd$_{44}$Ni$_{22}$}: a gigantic 3d−4f wheel-like nanoscale cluster with a large magnetocaloric effect†

Zixiu Lu, [ID] [a,b] Zhu Zhuo,[c,d] Wei Wang, [ID] *[c,d] You-Gui Huang*[c,d,e] and Maochun Hong [ID] [a,b,c,d]

Multinuclear 3d−4f nano-clusters, consisting of a large number of metal ions, are interesting both structurally and functionally. The Gd(III) containing clusters, in particular, attract great research attention because of their significant magnetocaloric effect. Here, we report the synthesis of a gigantic 3d−4f wheel-like cluster, {Gd$_{44}$Ni$_{22}$}, achieved through self-assembly using a "mixed-ligand" strategy. Magnetic characterization reveals that the {Gd$_{44}$Ni$_{22}$} cluster exhibits a large magnetocaloric effect (MCE), with an isothermal magnetic entropy change of 44.9 J kg^{-1} K^{-1} at 2.0 K for ΔH = 7 T, which is one of the largest among all of the high-nuclearity Ni−Gd clusters.

Introduction

High-nuclearity 3d–4f metal oxide/hydroxide clusters (M > 25) have attracted extensive research attention because of their fascinating structures and interesting properties.[1–10] Among the different properties, a particularly interesting one is the molecular magnetocaloric effect (MCE).[11–15] The MCE is a phenomenon that leads to a reversible temperature change when a material is exposed to a changing magnetic field.[16] The MCE is safe (without producing greenhouse gases), quiet, cheap, highly durable, and highly efficient (*i.e.* it requires only a small number of moving parts).[17] Currently, the greatest emphasis in the commercial use of MCE is on room temperature cooling (*e.g.* air conditioning, freezers, *etc.*). However, the cryogenic application of magnetic cooling materials will be increasingly important with the development of quantum computers,

which require ultra-low temperatures.[18,19] As a class of highly efficient refrigerants at cryogenic temperatures, molecular magnets are promising materials which exhibit a large MCE.[20,21]

Research reveals that metal oxide/hydroxide clusters displaying large MCEs share certain structural and functional features. These features include the high-spin ground state, large metal/ligand mass ratio (to ensure a high magnetic density), low-lying excited spin states, negligible magnetic anisotropy, and weak magnetic exchange coupling. Following this logic, research efforts on improving the MCE can be roughly divided into three categories. In the first category, 3d-clusters (*e.g.* {Fe$_{12}$} and {Mn$_8$}),[22–24] with high ground-state spin values, have been studied. However, strong magnetic coupling between transition metal ions results in antiferromagnetic interactions, leading to small MCEs. In the second category, studies have demonstrated larger MCEs in high-nuclearity Gd(III) oxide/hydroxide clusters. This is attributed to the Gd(III) ions with f^7 electron configuration, affording multiple low-lying excited spin states and a possible ground state with a large spin value.[25] For example, high-nuclearity Gd oxide/hydroxide clusters with large MCEs have been reported recently, including {Gd$_{60}$} (with the maximum magnetic entropy change ($-\Delta S_m$) of 48.0 J kg^{-1} K^{-1}),[12] {Gd$_{104}$} ($-\Delta S_m$ = 46.9 J kg^{-1} K^{-1}),[26] {Gd$_{48}$} ($-\Delta S_m$ = 43.6 J kg^{-1} K^{-1}),[27] *etc.* Finally, in the third category, Gd(III) ions have been exploited to mitigate the strong magnetic coupling between transition metal ions. By combining 3d metal ions and Gd(III), heterometallic 3d-Gd(III) clusters with small ligands turn out to be most promising for achieving a large MCE.[15] Heterometallic 3d-Gd(III) clusters with large MCEs have been reported in recent years, such as {Gd$_{102}$Ni$_{36}$} ($-\Delta S_m$ = 41.3 J kg^{-1} K^{-1}),[28] {Gd$_{96}$Ni$_{64}$} ($-\Delta S_m$ = 42.8 J kg^{-1} K^{-1}),[29] {Gd$_{78}$Ni$_{64}$} ($-\Delta S_m$ =

[a]Ganjiang Innovation Academy, Chinese Academy of Sciences, Ganzhou 341000, China
[b]School of Rare Earth, University of Science and Technology of China, Ganzhou, China
[c]CAS Key Laboratory of Design and Assembly of Functional Nanostructures, and Fujian Provincial Key Laboratory of Nanomaterials, Fujian Institute of Research on the Structure of Matter, Chinese Academy of Sciences, China.
E-mail: wangwei@fjirsm.ac.cn, yghuang@fjirsm.ac.c
[d]Xiamen Key Laboratory of Rare Earth Photoelectric Functional Materials, Xiamen Institute of Rare Earth Materials, Haixi Institutes, Chinese Academy of Sciences, Xiamen, Fujian 361021, China
[e]Fujian Science & Technology Innovation Laboratory for Optoelectronic Information of China, Fuzhou, 350108, China

This journal is © the Partner Organisations 2023

Inorg. Chem. Front., 2023, **10**, 979–983 | **979**

40.6 J kg^{-1} K^{-1}),[30] *etc.* Among different 3d-Gd(III) clusters, wheel-like clusters are less observed. To date, the only reported 3d-Gd wheel-like structures are {Gd$_{24}$Cu$_{36}$}[31] and {Gd$_{24}$Co$_{16}$},[32] both with small $-\Delta S_m$ of 21.0 J kg^{-1} K^{-1} and 26.0 J kg^{-1} K^{-1}, respectively. It is therefore important to obtain new heterometallic 3d-Gd(III) wheel-like clusters exhibiting a large MCE, to explore the relationship between the cluster structure and magnetocaloric effects.

In this work, a new wheel-like 3d-Gd(III) oxide/hydroxide cluster {Gd$_{44}$Ni$_{22}$} (**1**), with the formula [Gd$_{44}$Ni$_{22}$(CO$_3$)$_{16}$(NO$_3$)$_4$(H$_2$O)$_{58}$(μ_3-OH)$_{76}$(μ_2-OH)$_6$(IDA)$_{28}$(H$_2$dmpa)$_2$]·(H$_2$O)$_x$ (**1**, $x \approx 118$) (H$_2$dmp = 3-hydroxy-2-(hydroxymethyl)-2-methylpropanoic acid, IDA = iminodiacetic acid), is synthesized by using "mixed-ligands" to control the hydrolysis of Gd(III) and Ni(II) ions. The cluster structure and magnetic properties of **1** are investigated in detail to study the structure–property relationship to the magnetocaloric effects.

Results and discussion

Single crystals of the {Gd$_{44}$Ni$_{22}$} clusters (Fig. S1†) are obtained through the hydrolysis of Gd(NO$_3$)$_3$·6H$_2$O and Ni(NO$_3$)$_2$·6H$_2$O in the presence of mixed ligands {*i.e.*, iminodiacetic acid (IDA) and 2,2-dimethylol propionic acid (H$_3$dmpa)}. Single-crystal X-ray diffraction (Tables S1–S3†) reveals that {Gd$_{44}$Ni$_{22}$} crystallizes in the monoclinic space group $P2_1/n$, with the formula [Gd$_{44}$Ni$_{22}$(CO$_3$)$_{16}$(NO$_3$)$_4$(H$_2$O)$_{58}$(μ_3-OH)$_{76}$(μ_2-O)$_6$(IDA)$_{28}$(H$_2$dmpa)$_2$]·(H$_2$O)$_x$ (**1**, $x \approx 118$). The {Gd$_{44}$Ni$_{22}$} cluster features a novel giant wheel-like structure with an outer diameter of ~2.8 nm. The {Gd$_{44}$Ni$_{22}$} wheel also possesses an inner cavity, with the dimensions of 0.8 nm and 1.9 nm, respectively, in two perpendicular directions (Fig. 1).
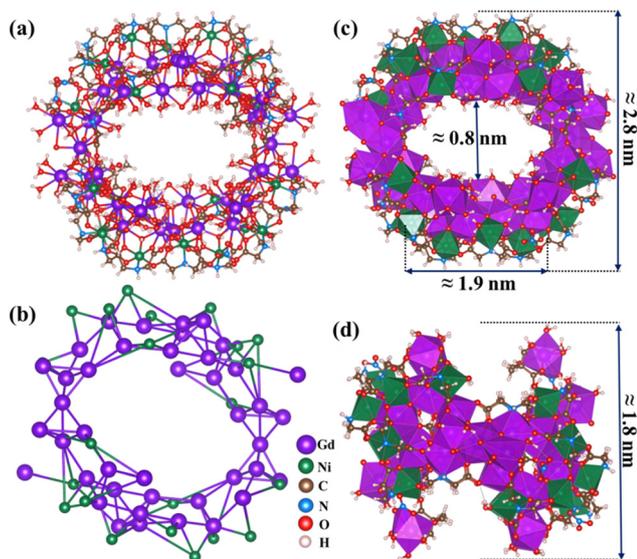
By taking a close look, we find that {Gd$_{44}$Ni$_{22}$} consists of one wheel-shaped {Gd$_{42}$Ni$_{22}$} unit (connected by μ_3-OH, CO$_3$$^{2-}$ and IDA ligands) and two Gd^{3+} ions (coordinated by NO$_3$$^-$ and H$_3$dmpa ligands). In the structure, the trivalent cations Gd^{3+} are eight-fold or nine-fold coordinated with O and N atoms, resulting in the [GdO$_9$], [GdO$_8$N], and [GdO$_8$] polyhedra (Fig. S2a, 5b, and 5c†). The Ni^{2+} ions are all six-coordinated with O and N atoms to form distorted [NiO$_5$N] octahedra (Fig. S2d†). The long distance between two neighboring metal ions (Gd···Gd = 3.618–3.971 Å and Gd···Ni = 3.452–3.538 Å) likely limits their magnetic interactions.

The wheel-shaped {Gd$_{42}$Ni$_{22}$} unit (Fig. 2a) consists of three different types of cluster subunits (I, II, and III). Subunit type I, formulated as [Gd$_7$(μ_3-OH)$_8$] (Fig. 2b), can be viewed as two cubane-like [Gd$_4$(μ_3-OH)$_4$] units that share a common Gd^{3+} vertex. Type II, formulated as [Gd$_{10}$Ni$_7$(μ_3-OH)$_{12}$(CO$_3$)$_2$] ({Gd$_{10}$Ni$_7$}), can be viewed as two CO$_3$$^{2-}$ templated five-member rings sharing a Gd^{3+} vertex while bridged by one additional Gd^{3+} ion (Fig. 2c). Here, CO$_3$$^{2-}$ likely originates from the absorption of atmospheric CO$_2$ by the reaction mixture, as observed by other researchers.[12,33] In addition, besides the CO$_3$$^{2-}$ ligands, the ten Gd^{3+} ions in each {Gd$_{10}$Ni$_7$} unit are connected by twelve hydroxo ligands, with seven Ni^{2+} ions distributed on the outer edge and connected to Gd^{3+} ions by μ_3-OH. Finally, subunit type III can be described as [Gd$_2$Ni$_2$(μ_3-OH)$_2$(CO$_3$)$_2$], with two Gd^{2+} and two Ni^{2+} connected by two μ_3-OH and two CO$_3$$^{2-}$ ligands (Fig. 2d). Two type I subunits, two type II subunits, and four type III subunits are joined together by sixteen CO$_3$$^{2-}$, eighty μ_3-OH, and two μ_2-O groups, forming the wheel-shaped {Gd$_{42}$Ni$_{22}$} component.

In the structure of {Gd$_{44}$Ni$_{22}$}, IDA and H$_3$dmpa have two functions: one is to link the type I, type II, and type III sub-
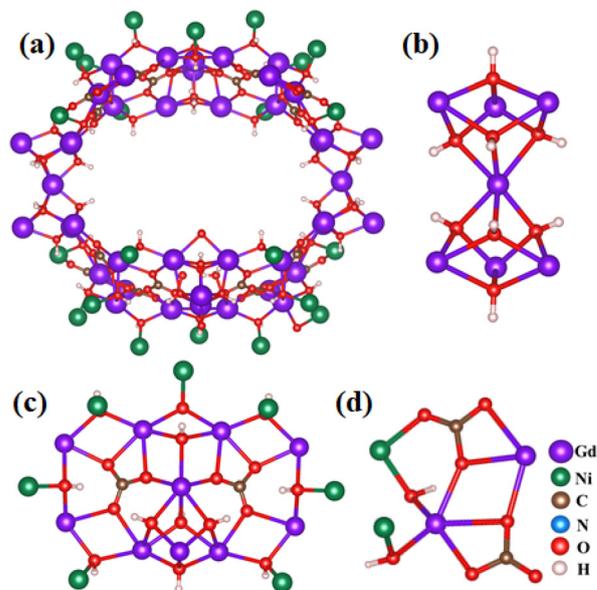

Fig. 1 (a) The structure of wheel-like {Gd$_{44}$Ni$_{22}$} cluster; (b) structure of the wheel-like geometry of {Gd$_{44}$Ni$_{22}$} consisting of 44 gadolinium and 22 nickel ions; polyhedron representation of the {Gd$_{44}$Ni$_{22}$} cluster (c) and (d). Color code: purple, Gd; green, Ni; red, O; gray, C; white, H.

Fig. 2 Ball-and-stick views of the assembly unit of the {Gd$_{44}$Ni$_{22}$} cluster. (a) {Gd$_{42}$Ni$_{22}$} units; (b) type I ([Gd$_7$(μ_3-OH)$_8$] unit); (c) type II ([Gd$_{10}$Ni$_7$(μ_3-OH)$_{12}$(CO$_3$)$_2$] unit); (d) type III ([Gd$_2$Ni$_2$(μ_3-OH)$_2$(CO$_3$)$_2$] unit).

980 | *Inorg. Chem. Front.*, 2023, **10**, 979–983

This journal is © the Partner Organisations 2023

units *via* coordination interactions and the other is to stabilize the wheel-shaped $\{Gd_{44}Ni_{22}\}$ core. The IDA^{2-} ligand coordinates to the Gd^{3+} and Ni^{2+} ions are of three types. The first type coordinates to two Gd^{3+} ions and three Ni^{2+} ions in a μ_5-$\eta_{Gd}^1(O):\eta_{Gd}^1(O):\eta_{Ni}^1(O):\eta_{Ni}^3(O,N,O):\eta_{Ni}^1(O)$ mode (Fig. 3a). The second type coordinates to three Gd^{3+} ions and two Ni^{2+} ions in a μ_5-$\eta_{Gd}^1(O):\eta_{Gd}^1(O):\eta_{Gd}^1(O):\eta_{Ni}^3(O,N,O):\eta_{Ni}^1(O)$ mode (Fig. 3b). The third type coordinates to three Gd^{3+} ions and two Ni^{2+} ions in a μ_5-$\eta_{Gd}^1(O):\eta_{Gd}^1(O):\eta_{Gd}^3(O,N,O):\eta_{Gd}^1(O):\eta_{Ni}^1(O)$ mode (Fig. 3c). Meanwhile, the H$_3$dmpa ligand coordinates to one Gd^{3+} and one Ni^{2+} in a μ_2-$\eta_{Gd}^3(O,O,O):\eta_{Ni}^1(O)$ mode (Fig. 3d). Structurally, the IDA ligand plays a key role in the formation of a wheel-shaped $\{Gd_{42}Ni_{22}\}$ unit. Two additional Gd^{3+} ions attach to the $\{Gd_{42}Ni_{22}\}$ unit only through H$_3$dmpa ligands, leading to the final $\{Gd_{44}Ni_{22}\}$ wheel. Interestingly, the packing of $\{Gd_{44}Ni_{22}\}$ clusters within the lattice results in a nanotube with a one-dimensional channel along the *a*-axis (Fig. S3†).

It is worth pointing out that high-nuclearity 3d–4f wheel-shaped nanoscale clusters with a large central opening are still underdeveloped. As far as we know, only $\{Cu_{36}^{II}Ln_{24}^{III}\}$ (Ln = Dy and Gd)[31] and $\{Co_{16}^{II}Ln_{24}^{III}\}$ (Ln = Dy and Gd)[32] clusters have been reported. $\{Cu_{36}^{II}Ln_{24}^{III}\}$ (Ln = Dy and Gd) consists of two alternating subunits (*i.e.* cubane-like [Ln$_4$(OH)$_4$] and boat-shaped [Cu$_6$(OH)$_8$(NO$_3$)]). The $\{Cu_{36}^{II}Ln_{24}^{III}\}$ wheel exhibits a diagonal dimension of ~4.6 nm, a thickness of about ~1.8 nm, and a central opening with a diameter of ~0.8 nm. Benzoate is involved in the formation of $\{Cu_{36}^{II}Ln_{24}^{III}\}$, as the primary linker and the protective ligand. Other wheel-shaped clusters, $\{Co_{16}^{II}Ln_{24}^{III}\}$ (Ln = Dy and Gd), have been successfully synthesized by adopting pyridyl-functionalized β-diketone as the ligand. The metallo-core of $\{Co_{16}Ln_{24}\}$ is constructed by a super-square $\{Ln_{24}\}$ with an octagonal prism $\{Co_{16}\}$. The diameter and thickness of the $\{Co_{16}^{II}Ln_{24}^{III}\}$ cluster are 3.0 nm and 2.0 nm, respectively. Clearly, the $\{Gd_{44}^{III}Ni_{22}^{II}\}$ cluster reported in this work represents a new type of high-nuclearity wheel-shaped cluster, with more metal atoms (44 gadolinium and 22 nickel atoms) than those in the previous examples.

The temperature dependence of direct-current (dc) magnetic susceptibility is characterized on $\{Gd_{44}Ni_{22}\}$ in an applied magnetic field of 1000 Oe and in the temperature
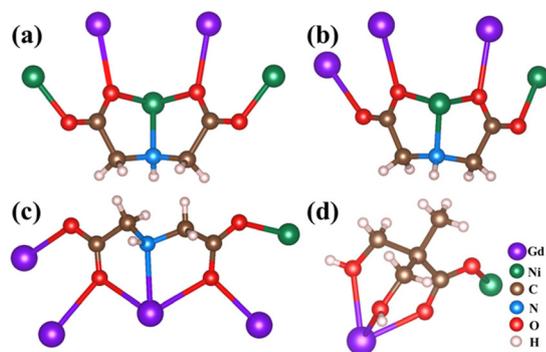
range 2–300 K. The characterization was performed on the polycrystalline powder samples (Fig. S4–S6†). As shown in Fig. S7,† the observed $\chi_m T$ value of 365.9 cm^3 K mol^{-1} (at 300 K) is slightly smaller than the theoretical value of 373.2 cm^3 K mol^{-1} calculated using the Lande formula[34,35] based on 22 uncorrelated Ni^{2+} ions (26.6 cm^3 K mol^{-1} for $S = 1$ and $g = 2.2$) and 44 uncorrelated Gd^{3+} ions (346.7 cm^3 K mol^{-1} for $S = 7/2$ and $g = 2$). This result confirms the limited interaction between these metal cations. The data over the temperature range of 2–300 K fit the Curie–Weiss law well, resulting in $C = 362.3$ cm^3 K mol^{-1} and $\theta = -5.3$ K for the $\{Gd_{44}Ni_{22}\}$ cluster. The negative θ further confirms the presence of weak antiferromagnetic interactions. This behavior might be ascribed to the weak exchange interactions between the metal ions (Ni⋯Ni, Ni⋯Gd, and Gd⋯Gd) *via* the bridging ligands.

The generally weak magnetic coupling between Gd^{3+} and 3d transition metal ions, benefiting from the ability of Gd^{3+} to mitigate the otherwise strong 3d–3d magnetic exchange, makes the 3d-Gd(III) clusters a valid class of materials for magnetic cooling applications. Here, the presence of a large number of Gd(III) ions in $\{Gd_{44}Ni_{22}\}$ prompts us to investigate its magnetocaloric effect in the context of developing molecular materials for magnetic cooling.[36,37] The field (H) dependence of the magnetization (M) of $\{Gd_{44}Ni_{22}\}$ at low temperature (2–10 K) is measured (Fig. 4a and Fig. S8†). The M *vs.* H data show a steady increase in magnetization, reaching 298.3$N\mu_B$ (N is the Avogadro constant and μ_B is the Bohr magneton) under 7 T at 2 K without achieving saturation (Fig. S8†). This value is slightly lower than the expected value for 66 uncorrelated metal ions (cal. 317.5$N\mu_B$). This again confirms the weak antiferromagnetic interactions in the cluster. The experimental maximum magnetic entropy change ($-\Delta S_m$) is calculated to be 44.9 J kg^{-1} K^{-1} at 2 K for $\Delta H = 7$ T using the Maxwell equation, $\Delta S_m(T) = \int [\partial M(T, H/\partial T)]_H dH$ (Fig. 4b). This experimental value is smaller than the theoretical value of 60.0 J kg^{-1} K^{-1} (based on the equation $S_m = R\ln(2S + 1)$ for 44 uncorrelated Gd^{3+} and 22 uncorrelated Ni^{2+} ions). The smaller experimental value might also be attributed to the presence of weak antiferromagnetic interactions.

It is worth noting that the $\{Gd_{44}Ni_{22}\}$ cluster demonstrates a large MCE, comparable to that of the recently reported high-nucleation cluster $\{Gd_{158}Co_{38}\}$[38] ($-\Delta S_m = 46.95$ J kg^{-1} K^{-1} at 2.0 K for $\Delta H = 7$ T). It is also significantly larger than that of other wheel-like 3d-Gd(III) clusters (Table S4†), such as $\{Gd_{24}Co_{16}\}$[32] ($-\Delta S_m = 26.0$ J kg^{-1} K^{-1} at 3.8 K for $\Delta H = 7$ T) and $\{Gd_{24}Cu_{36}\}$[31] ($-\Delta S_m = 21.0$ J kg^{-1} K^{-1}). Meanwhile, the MCE of **1** is also among the largest when compared with the reported homometallic Gd-clusters (Table S4†), demonstrating its great potential for magnetic cooling.

The large MCE of $\{Gd_{44}Ni_{22}\}$ may be attributed to the following reasons: first, by using ligands with a large number of coordination sites and minor steric hindrances, such as IDA and H$_3$dmpa, we are able to bond and stabilize a large number of metal ions in a relatively compact fashion. This results in a large metal/ligand ratio to ensure a high magnetic density for the large MCE. Second, Gd^{3+} effectively increases the distance

Fig. 3 Coordination modes of the IDA ligand (a–c); coordination mode of the H$_3$ dmpa ligand.

This journal is © the Partner Organisations 2023

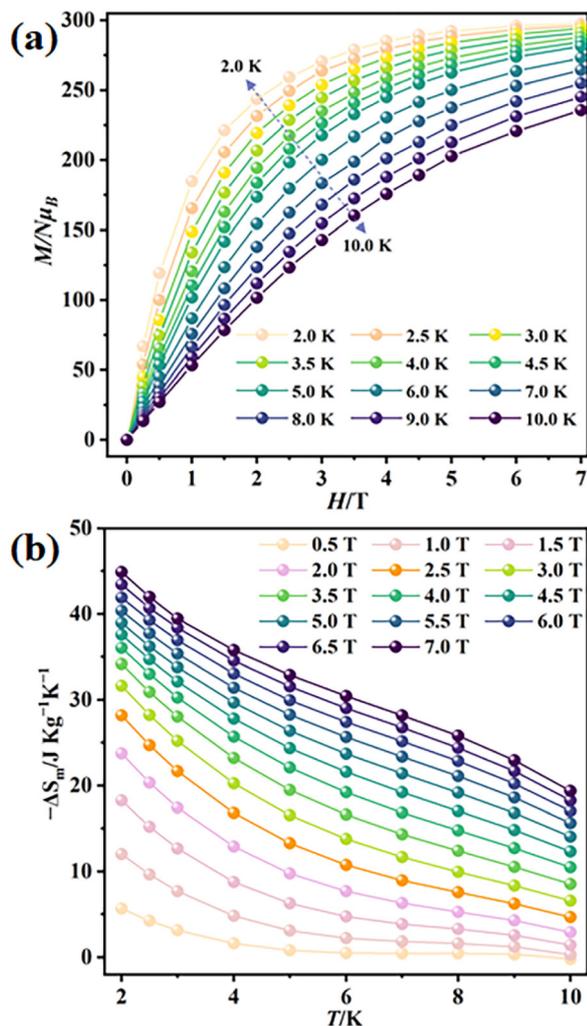*Inorg. Chem. Front.*, 2023, **10**, 979–983 | **981**

Fig. 4 (a) Field dependence of isothermal normalized magnetizations at 2–10 K; (b) plots of experimental magnetic entropy change ($-\Delta S_m$) vs. temperature (T) of the wheel-like {Gd$_{44}$Ni$_{22}$} cluster.

between Ni^{2+} ions (i.e., to 5.195–5.272 Å), and hence reduces the magnetic coupling between adjacent Ni^{2+} ions. Still, we notice weak antiferromagnetic couplings in **1** (θ = −5.3 K), indicating that further structural tuning might help to avoid the magnetic interaction and further enhance the MCE of **1**.

Conclusion

In summary, a novel wheel-like 3d-Gd cluster, {Gd$_{44}$Ni$_{22}$}, is synthesized by adopting the "mixed-ligand" strategy. As a promising magnetic cooling material, {Gd$_{44}$Ni$_{22}$} demonstrates a large MCE, with $-\Delta S_m$ of 44.9 J kg^{-1} K^{-1} at 2 K under 7 T. This value is one of the highest among all known high-nuclearity 3d–4f clusters. The large MCE is caused by the high metal/ligand ratio, which leads to high magnetic density. Further studies on tuning the cluster structure to reduce anti-ferromagnetic interactions and enhance the MCE of **1** are

underway and will be reported in our forthcoming contribution.

Conflicts of interest

There are no conflicts to declare.

Acknowledgements

References

1 T. Liu, E. Diemann, H. Li, A. W. M. Dress and A. Müller, Self-assembly in aqueous solution of wheel-shaped Mo154 oxide clusters into vesicles, *Nature*, 2003, **426**, 59–62.

2 I. Colliard, J. C. Brown, D. B. Fast, A. K. Sockwell, A. E. Hixon and M. Nyman, Snapshots of Ce70 toroid assembly from solids and solution, *J. Am. Chem. Soc.*, 2021, **143**, 9612–9621.

3 B. Russell-Webster, J. Lopez-Nieto, K. A. Abboud and G. Christou, Truly monodisperse molecular nanoparticles of cerium dioxide of 2.4 nm dimensions: A {Ce100O167} cluster, *Angew. Chem., Int. Ed.*, 2021, **60**, 12591–12596.

4 X. X. Hang, B. Liu, X. F. Zhu, S. T. Wang, H. T. Han, W. P. Liao, Y. L. Liu and C. H. Hu, Discrete {Ni40} coordination cage: A calixarene-based Johnson-Type (J17) hexadecahedron, *J. Am. Chem. Soc.*, 2016, **138**, 2969–2972.

5 C. D. Wu, C. Z. Lu, H. H. Zhuang and J. S. Huang, Hydrothermal assembly of a novel three-dimensional framework formed by [GdMo$_{12}$O$_{42}$]$_9^-$ anions and nine co-ordinated GdIII cations, *J. Am. Chem. Soc.*, 2002, **124**, 3836–3837.

6 X. M. Luo, S. Huang, P. Luo, K. Ma, Z. Y. Wang, X. Y. Dong and S. Q. Zang, Snapshots of key intermediates unveiling the growth from silver ions to Ag70 nanoclusters, *Chem. Sci.*, 2022, **13**, 11110–11118.

7 Y. F. Bi, X. T. Wang, W. P. Liao, X. F. Wang, X. W. Wang and H. J. Zhang, A {Co32} nanosphere supported by p-tert-butylthiacalix[4]arene, *J. Am. Chem. Soc.*, 2009, **131**, 11650–11651.

8 E. G. Ribó, N. L. Bell, W. M. Xuan, J. C. Luo, D. L. Long, T. B. Liu and L. Cronin, Synthesis, assembly, and sizing of neutral, lanthanide substituted molybdenum blue wheels {Mo90Ln10}, *J. Am. Chem. Soc.*, 2020, **142**, 17508–17514.

982 | *Inorg. Chem. Front.*, 2023, **10**, 979–983

This journal is © the Partner Organisations 2023

9 S. Kenzler and A. Schnepf, Metalloid gold clusters – Past, current and future aspects, *Chem. Sci.*, 2021, **12**, 3116–3129.

10 Z. G. Jiang, W. H. Wu, B. X. Jin, H. M. Zeng, Z. G. Jin and C. H. Zhan, A chloride-doped silver-sulfide cluster [Ag$_{148}$S$_{26}$Cl$_{30}$ (C=CBut)60]$^{6+}$: Hierarchical assembly, enhanced luminescence and cytotoxicity to cancer cells, *Nanoscale*, 2022, **14**, 1971–1977.

11 L. Qin, Y. Z. Yu, P. Q. Liao, W. Xue, Z. P. Zheng, X. M. Chen and Y. Z. Zheng, A "molecular water pipe": A giant tubular cluster {Dy72} exhibits fast proton transport and slow magnetic relaxation, *Adv. Mater.*, 2016, **28**, 10772–10779.

12 X. M. Luo, Z. B. Hu, Q. F. Lin, W. W. Cheng, J. P. Cao, C. H. Cui, H. Mei, Y. Song and Y. Xu, Exploring the performance improvement of magnetocaloric effect based Gd-exclusive cluster Gd60, *J. Am. Chem. Soc.*, 2018, **140**, 11219–11222.

13 H. J. Lun, L. Xu, X. J. Kong, L. S. Long and L. S. Zheng, A high-symmetry double-shell Gd$_{30}$Co$_{12}$ cluster exhibiting a large magnetocaloric effect, *Inorg. Chem.*, 2021, **60**, 10079–10083.

14 V. Corradini, A. Ghirri, A. Candini, R. Biagi, U. D. Pennino, G. Dotti, E. Otero, F. Choueikani, R. J. Blagg, E. J. L. McInnes and M. Affronte, Magnetic cooling at a single molecule level: a spectroscopic investigation of isolated molecules on a surface, *Adv. Mater.*, 2013, **25**, 2816–2820.

15 J. B. Peng, Q. C. Zhang, X. J. Kong, Y. Z. Zheng, Y. P. Ren, L. S. Long, R. B. Huang, L. S. Zheng and Z. P. Zheng, High-nuclearity 3d–4f clusters as enhanced magnetic coolers and molecular magnets, *J. Am. Chem. Soc.*, 2012, **134**, 3314–3317.

16 P. Konieczny, W. Sas, D. Czernia, A. Pacanowska, M. Fitta and R. Pełka, Magnetic cooling: A molecular perspective, *Dalton Trans.*, 2022, **51**, 12762–12780.

17 X. Y. Zheng, X. J. Kong, Z. P. Zheng, L. S. Long and L. S. Zheng, High-nuclearity lanthanide-containing clusters as potential molecular magnetic coolers, *Acc. Chem. Res.*, 2018, **51**, 517–525.

18 E. Warburg, Magnetische untersuchungen, *Ann. Phys.*, 1881, **249**, 141–164.

19 P. Debye, Einige Bemerkungen zur Magnetisierung bei tiefer Temperatur, *Ann. Phys.*, 1926, **386**, 1154–1160.

20 W. F. Giauque, A thermodynamic treatment of certain magnetic effects. A proposed method of producing temperatures considerably below 1 absolute, *J. Am. Chem. Soc.*, 1927, **49**, 1864–1870.

21 O. Tegus, E. Bruck, K. H. J. Buschow and F. R. de Boer, Transition-metal-based magnetic refrigerants for room-temperature applications, *Nature*, 2002, **415**, 150–152.

22 F. Torres, J. M. Hernández, X. Bohigas and J. Tejada, Giant and time-dependent magnetocaloric effect in high-spin molecularmagnets, *Appl. Phys. Lett.*, 2000, **77**, 3248–3250.

23 T. Lis, Preparation, structure, and magnetic properties of a dodecanuclear mixed-valence manganese carboxylate, *Acta Crystallogr., Sect. B: Struct. Crystallogr. Cryst. Chem.*, 1980, **36**, 2042.

24 D. Gatteschi, A. Caneschi, L. Pardi and R. Sessoli, Large clusters of metal ions: The transition from molecular to bulk magnets, *Science*, 1994, **265**, 1054.

25 J. W. Sharples, Y. Z. Zheng, F. Tuna, E. J. McInnes and D. Collison, Lanthanide discs chill well and relax slowly, *Chem. Commun.*, 2011, **47**, 7650–7652.

26 J. B. Peng, X. J. Kong, Q. C. Zhang, M. Orendac, J. Prokleska, Y. P. Ren, L. S. Long, Z. Zheng and L. S. Zheng, Beauty, symmetry, and magnetocaloric effect four-shell keplerates with 104 lanthanide atoms, *J. Am. Chem. Soc.*, 2014, **136**, 17938–17941.

27 F. S. Guo, Y. C. Chen, L. L. Mao, W. Q. Lin, J. D. Leng, R. Tarasenko, M. Orendáč, J. Prokleška, V. Sechovsky and M. L. Tong, Anion-templated assembly and magnetocaloric properties of a nanoscale {Gd38} cage versus a {Gd48} barrel, *Chem. – Eur. J.*, 2013, **19**, 14876–14885.

28 W. P. Chen, P. Q. Liao, P. B. Jin, L. Zhang, B. K. Ling, S. C. Wang, Y. T. Chan, X. M. Chen and Y. Z. Zheng, The gigantic {Ni$_{36}$Gd$_{102}$} hexagon: A sulfate-templated "star-of-David" for photocatalytic CO$_2$ reduction and magnetic cooling, *J. Am. Chem. Soc.*, 2020, **142**, 4663–4670.

29 W. P. Chen, P. Q. Liao, Y. Yu, Z. Zheng, X. M. Chen and Y. Z. Zheng, A mixed–ligand approach for a gigantic and hollow heterometallic cage {Ni$_{64}$RE$_{96}$} for gas separation and magnetic cooling applications, *Angew. Chem., Int. Ed.*, 2016, **55**, 9375–9379.

30 Q. F. Lin, J. Li, X. M. Luo, C. H. Cui, Y. Song and Y. Xu, Incorporation of silicon–oxygen tetrahedron into novel high-nuclearity nanosized 3d–4f heterometallic clusters, *Inorg. Chem.*, 2018, **57**, 4799–4802.

31 J. D. Leng, J. L. Liu and M. L. Tong, Unique nanoscale {Cu^{II} 36 Ln^{III} 24}(Ln = Dy and Gd) metallo-rings, *Chem. Commun.*, 2012, **48**, 5286–5288.

32 Z. M. Zhang, L. Y. Pan, W. Q. Lin, J. D. Leng, F. S. Guo, Y. C. Chen, J. L. Liu and M. L. Tong, Wheel-shaped nanoscale 3d–4f {Co II 16 Ln III 24} clusters (Ln = Dy and Gd), *Chem. Commun.*, 2013, **49**, 8081–8083.

33 X. Y. Zheng, Y. H. Jiang, G. L. Zhuang, D. P. Liu, H. G. Liao, X. J. Kong, L. S. Long and L. S. Zheng, A gigantic molecular wheel of {Gd140}: A new member of the molecular Wheel Family, *J. Am. Chem. Soc.*, 2017, **139**, 18178–18181.

34 C. Benelli and D. Gatteschi, Magnetism of lanthanides in molecular materials with transition-metal ions and organic radicals, *Chem. Rev.*, 2002, **102**, 2369.

35 O. Kahn, *Molecular Magnetism*, VCH, New York, 1993.

36 Y. Z. Zheng, G. J. Zhou, Z. Zheng and R. E. P. Winpenny, Molecule-based magnetic coolers, *Chem. Soc. Rev.*, 2014, **43**, 1462–1475.

37 J. L. Liu, Y. C. Chen, F. S. Guo and M. L. Tong, Recent advances in the design of magnetic molecules for use as cryogenic magnetic coolants, *Coord. Chem. Rev.*, 2014, **281**, 26–49.

38 N. F. Li, X. M. Min, J. Wang, J. L. Wang, Y. Song, H. Mei and Y. Xu, Largest 3d–4f 196-nuclear Gd$_{158}$Co$_{38}$ clusters with excellent magnetic cooling, *Sci. China: Chem.*, 2022, **65**, 1577–1583.

This journal is © the Partner Organisations 2023

Inorg. Chem. Front., 2023, **10**, 979–983 | **983**